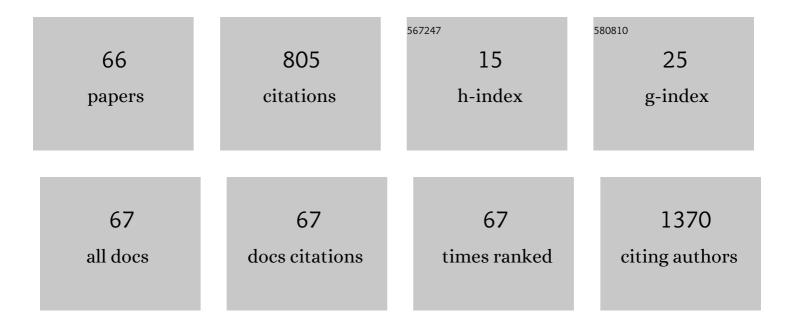
List of Publications by Year in descending order

Source: https://exaly.com/author-pdf/5966542/publications.pdf Version: 2024-02-01



Ηγιινίος Shin

#	Article	IF	CITATIONS
1	Localized cystic disease of the kidney in pediatric patients: Clinical and imaging findings with long term follow up. Journal of Pediatric Urology, 2022, 18, 90.e1-90.e8.	1.1	0
2	Initial Abdominal CT and Laboratory Findings Prior to Diagnosis of Crohn's Disease in Children. Yonsei Medical Journal, 2022, 63, 675.	2.2	0
3	Diagnostic performance of artificial intelligence approved for adults for the interpretation of pediatric chest radiographs. Scientific Reports, 2022, 12, .	3.3	10
4	Successful Implementation of an Artificial Intelligence-Based Computer-Aided Detection System for Chest Radiography in Daily Clinical Practice. Korean Journal of Radiology, 2022, 23, 847.	3.4	16
5	Prediction of postinfectious bronchiolitis obliterans prognosis in children. Pediatric Pulmonology, 2021, 56, 1069-1076.	2.0	5
6	Differentiation between Clear Cell Sarcoma of the Kidney and Wilms' Tumor with CT. Korean Journal of Radiology, 2021, 22, 1185.	3.4	9
7	Diffusion-Weighted Imaging for Differentiation of Biliary Atresia and Grading of Hepatic Fibrosis in Infants with Cholestasis. Korean Journal of Radiology, 2021, 22, 253.	3.4	3
8	Quantitative MRI Assessment of Pancreatic Steatosis Using Proton Density Fat Fraction in Pediatric Obesity. Korean Journal of Radiology, 2021, 22, 1886.	3.4	7
9	Establishment of Local Diagnostic Reference Levels of Pediatric Abdominopelvic and Chest CT Examinations Based on the Body Weight and Size in Korea. Korean Journal of Radiology, 2021, 22, 1172.	3.4	5
10	Bedside upper gastrointestinal series in the neonatal intensive care unit. BMC Pediatrics, 2021, 21, 91.	1.7	0
11	Children's Hepatic Tumors International Collaboration-Hepatoblastoma Stratification (CHIC-HS) System for Pediatric Patients with Hepatoblastoma: A Retrospective, Hospital-Based Cohort Study in South Korea. Cancer Research and Treatment, 2021, , .	3.0	1
12	Key imaging features for differentiating cystic biliary atresia from choledochal cyst: prenatal ultrasonography and postnatal ultrasonography and MRI. Ultrasonography, 2021, 40, 301-311.	2.3	14
13	Outcome of staging chest CT and identification of factors associated with lung metastasis in children with hepatoblastoma. European Radiology, 2021, 31, 8850-8857.	4.5	4
14	Painful Hashimoto Thyroiditis in a 7-Year-Old Girl: Differential Diagnosis and Medical Treatment. International Journal of Thyroidology, 2021, 14, 50-54.	0.1	0
15	High Prevalence of Nonalcoholic Fatty Liver Disease Among Adolescents and Young Adults With Hypopituitarism due to Growth Hormone Deficiency. Endocrine Practice, 2021, 27, 1149-1155.	2.1	11
16	Effect of different driver power amplitudes on liver stiffness measurement in pediatric liver MR elastography. Abdominal Radiology, 2021, 46, 4729-4735.	2.1	2
17	Renal growth slope in children with congenital and acquired solitary functioning kidneys. Ultrasonography, 2021, 40, 357-365.	2.3	1
18	Psoas muscle area and paraspinal muscle fat in children and young adults with or without obesity and fatty liver. PLoS ONE, 2021, 16, e0259948.	2.5	1

#	Article	IF	CITATIONS
19	Renal elasticity and perfusion changes associated with fibrosis on ultrasonography in a rabbit model of obstructive uropathy. European Radiology, 2020, 30, 1986-1996.	4.5	11
20	Bone marrow fat change in pediatric patients with non-alcoholic fatty liver disease. PLoS ONE, 2020, 15, e0234096.	2.5	4
21	Hepatic subcapsular or capsular flow in biliary atresia: is it useful imaging feature after the Kasai operation?. European Radiology, 2020, 30, 3161-3167.	4.5	7
22	Liver stiffness and perfusion changes for hepatic sinusoidal obstruction syndrome in rabbit model. World Journal of Gastroenterology, 2020, 26, 706-716.	3.3	10
23	Periportal thickening on magnetic resonance imaging for hepatic fibrosis in infantile cholestasis. World Journal of Gastroenterology, 2020, 26, 2821-2830.	3.3	5
24	Imaging of Acute Pulmonary and Airway Diseases in Children. Journal of the Korean Society of Radiology, 2020, 81, 756.	0.2	0
25	Determining the optimal timing of screening spinal cord ultrasonography to detect filum terminale lipoma in infants. Ultrasonography, 2020, 39, 367-375.	2.3	1
26	Normal Changes and Ranges of Pediatric Testicular Volume and Shear Wave Elasticity. Ultrasound in Medicine and Biology, 2019, 45, 1638-1643.	1.5	6
27	Texture Analysis to Differentiate Malignant Renal Tumors in Children Using Gray-Scale Ultrasonography Images. Ultrasound in Medicine and Biology, 2019, 45, 2205-2212.	1.5	7
28	Quick assessment with controlled attenuation parameter for hepatic steatosis in children based on MRI-PDFF as the gold standard. BMC Pediatrics, 2019, 19, 112.	1.7	38
29	Quantitative CT and pulmonary function in children with post-infectious bronchiolitis obliterans. PLoS ONE, 2019, 14, e0214647.	2.5	16
30	Performance of deep learning-based algorithm for detection of ileocolic intussusception on abdominal radiographs of young children. Scientific Reports, 2019, 9, 19420.	3.3	11
31	Clinical utility of mono-exponential model diffusion weighted imaging using two b-values compared to the bi- or stretched exponential model for the diagnosis of biliary atresia in infant liver MRI. PLoS ONE, 2019, 14, e0226627.	2.5	10
32	Feasibility of Spin-Echo Echo-Planar Imaging MR Elastography in Livers of Children and Young Adults. Investigative Magnetic Resonance Imaging, 2019, 23, 251.	0.4	2
33	Quantitative Imaging in Pediatric Hepatobiliary Disease. Korean Journal of Radiology, 2019, 20, 1342.	3.4	13
34	Predicting gastroesophageal varices through spleen magnetic resonance elastography in pediatric liver fibrosis. World Journal of Gastroenterology, 2019, 25, 367-377.	3.3	26
35	Title is missing!. , 2019, 14, e0226627.		0

#	Article	IF	CITATIONS
37	Title is missing!. , 2019, 14, e0226627.		Ο
38	Title is missing!. , 2019, 14, e0226627.		0
39	MRI-based decision tree model for diagnosis of biliary atresia. European Radiology, 2018, 28, 3422-3431.	4.5	37
40	Liver intravoxel incoherent motion diffusion-weighted imaging for the assessment of hepatic steatosis and fibrosis in children. World Journal of Gastroenterology, 2018, 24, 3013-3020.	3.3	19
41	Motion effects on the measurement of stiffness on ultrasound shear wave elastography: a moving liver fibrosis phantom study. Medical Ultrasonography, 2018, 1, 14.	0.8	8
42	Interconversion of elasticity measurements between two-dimensional shear wave elastography and transient elastography. Medical Ultrasonography, 2018, 20, 127.	0.8	9
43	Simplified split-bolus intravenous contrast injection technique for pediatric abdominal CT. Clinical Imaging, 2017, 46, 28-32.	1.5	3
44	Lung Clearance Index and Quantitative Computed Tomography of Post-Infectious Bronchiolitis Obliterans in Infants. Scientific Reports, 2017, 7, 15128.	3.3	11
45	Predicting lymph node metastasis in patients with papillary thyroid carcinoma by vascular index on power Doppler ultrasound. Head and Neck, 2017, 39, 334-340.	2.0	11
46	Testicular volume and elasticity changes in young children with undescended testes. Medical Ultrasonography, 2017, 19, 380.	0.8	13
47	Botryoid Wilms' Tumor in a Child Presenting with Gross Hematuria: A Case Report. Journal of the Korean Society of Radiology, 2016, 75, 198.	0.2	2
48	Imaging Features of Infratentorial Desmoplastic Infantile and Non-Infantile Tumors. Journal of the Korean Society of Radiology, 2016, 75, 49.	0.2	0
49	Comparison of effective radiation doses from X-ray, CT, and PET/CT in pediatric patients with neuroblastoma using a dose monitoring program. Diagnostic and Interventional Radiology, 2016, 22, 390-394.	1.5	27
50	Optimal Acquisition Number for Hepatic Shear Wave Velocity Measurements in Children. PLoS ONE, 2016, 11, e0168758.	2.5	26
51	Superb microvascular imaging for the detection of parenchymal perfusion in normal and undescended testes in young children. European Journal of Radiology, 2016, 85, 649-656.	2.6	47
52	Comparison of shear wave velocities on ultrasound elastography between different machines, transducers, and acquisition depths: a phantom study. European Radiology, 2016, 26, 3361-3367.	4.5	89
53	Imaging patterns of sonographic lenticulostriate vasculopathy and correlation with clinical and neurodevelopmental outcome. Journal of Clinical Ultrasound, 2015, 43, 367-374.	0.8	12
54	Pathological Evaluation of Radiation-Induced Vascular Lesions of the Brain: Distinct from <i>De Novo</i> Cavernous Hemangioma. Yonsei Medical Journal, 2015, 56, 1714.	2.2	25

#	Article	IF	CITATIONS
55	Normal Range of Hepatic Fat Fraction on Dual- and Triple-Echo Fat Quantification MR in Children. PLoS ONE, 2015, 10, e0117480.	2.5	15
56	Radiation dose and image quality in pediatric chest CT: effects of iterative reconstruction in normal weight and overweight children. Pediatric Radiology, 2015, 45, 337-344.	2.0	21
57	Quantitative computed tomography assessment of graft-versus-host disease-related bronchiolitis obliterans in children: A pilot feasibility study. European Radiology, 2015, 25, 2931-2936.	4.5	9
58	Quantitative Evaluation of Vascularity Using 2-D Power Doppler Ultrasonography May Not Identify Malignancy of the Thyroid. Ultrasound in Medicine and Biology, 2015, 41, 2873-2883.	1.5	6
59	Optimal Filum Terminale Thickness Cutoff Value on Sonography for Lipoma Screening in Young Children. Journal of Ultrasound in Medicine, 2015, 34, 1943-1949.	1.7	13
60	Prepubertal Testicular Teratomas and Epidermoid Cysts. Journal of Ultrasound in Medicine, 2015, 34, 1745-1751.	1.7	12
61	A Study on Serum Antithyroglobulin Antibodies Interference in Thyroglobulin Measurement in Fine-Needle Aspiration for Diagnosing Lymph Node Metastasis in Postoperative Patients. PLoS ONE, 2015, 10, e0131096.	2.5	15
62	Hepatic fat quantification magnetic resonance for monitoring treatment response in pediatric nonalcoholic steatohepatitis. World Journal of Gastroenterology, 2015, 21, 9741.	3.3	8
63	Contrast-enhanced ultrasonography for the evaluation of liver fibrosis after biliary obstruction. World Journal of Gastroenterology, 2015, 21, 2614.	3.3	5
64	Differentiation between Primary Cerebral Lymphoma and Glioblastoma Using the Apparent Diffusion Coefficient: Comparison of Three Different ROI Methods. PLoS ONE, 2014, 9, e112948.	2.5	54
65	Can increased tumoral vascularity be a quantitative predicting factor of lymph node metastasis in papillary thyroid microcarcinoma?. Endocrine, 2014, 47, 273-282.	2.3	21
66	Radiation Dose Reduction via Sinogram Affirmed Iterative Reconstruction and Automatic Tube Voltage Modulation (CARE kV) in Abdominal CT. Korean Journal of Radiology, 2013, 14, 886.	3.4	31